Soils and Foundations 2015;55(1):166–180

HOSTED BY

ELSEVIER

CrossMark

The Japanese Geotechnical Society

Soils and Foundations

www.sciencedirect.com
journal homepage: www.elsevier.com/locate/sandf

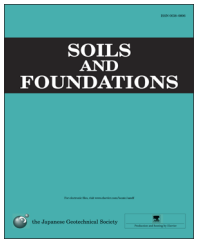

Effect of shrinkage on air-entry value of soils

M. Wijaya, E.C. Leong*, H. Rahardjo

School of Civil & Environmental Engineering, Nanyang Technological University, Blk N1, 50 Nanyang Avenue, Singapore 639798, Singapore

Received 31 December 2013; received in revised form 3 September 2014; accepted 21 October 2014
Available online 1 January 2015

Abstract

The soil–water characteristic curve (SWCC) is an important property of unsaturated soils. One key parameter of the SWCC is the air-entry value. For a soil that does not shrink as soil suction increases, the air-entry value is the same regardless of whether the gravimetric water content-based SWCC (SWCC-w), the volumetric water content-based SWCC (SWCC-θ) or the degree of saturation-based SWCC (SWCC-S) is used. However, for a soil that shrinks as soil suction increases, the air-entry value depends on the SWCC. The air-entry value determined from the SWCC-w is shown to underestimate the air-entry value for a soil that shows shrinkage as soil suction increases. For such cases, the SWCC-S should be used to determine the air-entry value. The SWCC-S can be constructed using the SWCC-w and the shrinkage curve. The shrinkage curve provides the void ratio and the water content for calculating the degree of saturation which can then be used to transform the SWCC-w to the SWCC-S. The shrinkage curve can be easily constructed from the final volume measurement of a drying soil specimen, as shown in this paper. The sensitivity analyses performed on 40 soils showed that the minimum void ratio of the shrinkage curve (a_{sh}) has a very significant effect, while the curvature of the shrinkage curve (c_{sh}) has a negligible effect on the SWCC-S, and therefore, on the determination of the AEV. A procedure is proposed for determining the air-entry value of soils exhibiting shrinkage upon drying.

Keywords: Shrinkage; Soil–water characteristic curve; Air-entry value; Water content; Degree of saturation; Unsaturated soil

1. Introduction

In the application of unsaturated soil mechanics, the engineering properties of unsaturated soils are required. However, the test duration for unsaturated soils is several times longer than that for equivalent saturated soil tests. To alleviate the problem of the long unsaturated soil test duration in geotechnical engineering practice, the soil–water characteristic curve (SWCC) has been heavily utilized to determine the unsaturated soil properties indirectly. The SWCC is the relationship between the soil–water content (by mass or volume) and the soil–water matric potential (Leong and Rahardjo, 1997). One key parameter of the SWCC is the air-entry value (AEV) which demarcates the change from boundary effect zone to transition effect zone, as shown in Fig. 1. The AEV is defined as the matric suction where air starts to enter the largest pores in the soil (Fredlund and Xing, 1994). The AEV appears in many equations used to estimate unsaturated soil properties, such as the shear strength (e.g., Bao et al., 1998; Goh et al., 2010; Khalili and Khabbaz, 1998; Lee et al., 2005; Rassam and Cook, 2002; Rassam and Williams, 1999; Tekinsoy et al., 2004; Xu, 2004) and the permeability function (e.g., Hunt, 2004; Mbonimpa et al., 2006; Philip, 1986; Rijtema, 1965; Watabe and Leroueil, 2006).

In Fig. 1, the ordinate axis labelled "water content" can be either gravimetric water content w, volumetric water content θ or degree of saturation S. Fredlund et al. (2001) suggested that the same information in the SWCC is conveyed regardless of the term used to describe the water content provided that the

*Corresponding author. Tel.: +65 6790 4774; fax +65 6791 0676.
E-mail address: cecleong@ntu.edu.sg (E.C. Leong).
Peer review under responsibility of The Japanese Geotechnical Society.

http://dx.doi.org/10.1016/j.sandf.2014.12.013

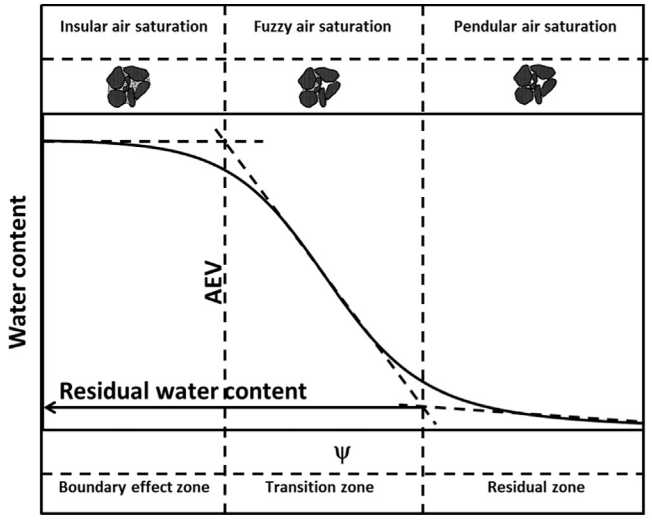

Fig. 1. Soil–water characteristic curve and parameters adopted from Kohgo (2003).

structure of the soil is incompressible. If the soil shrinks, as a result of an increase in soil suction, the AEV should be obtained from the SWCC where the ordinate axis is the degree of saturation, i.e., the SWCC-*S*. In agriculture-related disciplines, the volumetric water content is commonly used to plot the SWCC. The volumetric water content is defined as the volume of water in the soil referenced to the instantaneous total volume of the soil. However, it is quite common to use the initial total volume of the soil to determine the volumetric water content (Fredlund et al., 2011). If this is the case, both SWCCs, where the ordinate axis is the gravimetric water content (SWCC-*w*) and where the ordinate axis is the volumetric water content (SWCC-θ), show similar information. The use of the SWCC-θ is ambiguous as it may be plotted with the volume of water in the soil referenced to the initial total volume or the instantaneous total volume of the soil. In geotechnical engineering, the gravimetric water content is commonly used to describe the amount of water in the soil, and it should be used to plot the soil–water characteristic curve when continuous volume measurements have not been made (Fredlund et al., 2001).

Some soils undergo volume change as their water content changes. The relationship between the gravimetric water content (w) and the void ratio (e) is known as the shrinkage curve. Fredlund et al. (2011) has shown that the SWCC-*S* can be constructed using the shrinkage curve and the SWCC-*w*. Ignoring the shrinkage curve and using only the SWCC-*w* to determine the AEV will underestimate the AEV of the soil. There are at least two important parameters in describing the shrinkage curve (Fredlund et al., 2002). The first is the minimum void ratio (e_{min}) and the second is the curvature of the shrinkage curve. In practice, it is usually very difficult to accurately measure the volume of a soil during the SWCC test (Peron et al., 2007; Liu et al., 2012). Some reasons are due to the non-homogenous shrinkage and cracks that may occur during the drying process, as shown in Fig. 2. Fredlund et al. (2002) proposed to estimate the minimum void ratio by using

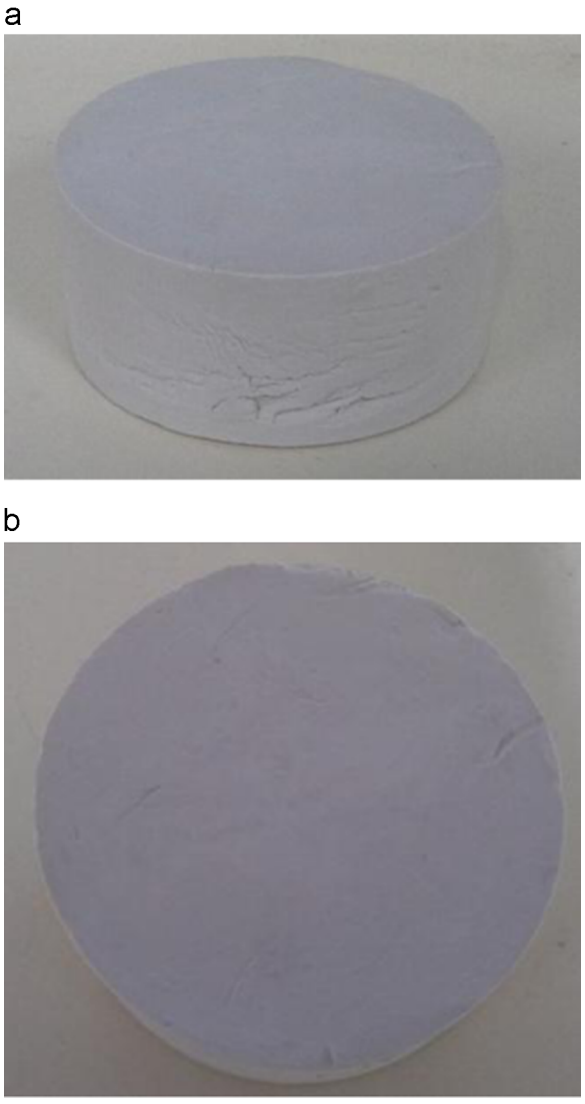

Fig. 2. Cracks and non-uniform deformation in a kaolin specimen that cause uncertainty in volume measurement. (a) Crack appears at the side of the soil specimen and causes inaccuracy in the volume measurement and (b) Non-uniform deformation at the perimeter of the specimen causes a lot of difficulty in measuring the volume.

the shrinkage limit. However, the accuracy and the sensitivity of the minimum void ratio and the curvature of the shrinkage curve on the AEV are not clearly understood. The objective of this paper is to investigate the effect of shrinkage on the determination of the AEV. Forty soils from the literature and the SoilVision (2003) database were used to analyse the effect of the shrinkage curve parameters (minimum void ratio and curvature of the shrinkage curve) on the AEV of soils. Shrinkage tests on kaolin specimens were then conducted to illustrate the effect of the shrinkage curve on the AEV.

2. Shrinkage curve

In order to construct the SWCC-*S*, the shrinkage curve is needed. When a soil is saturated, the reduction in void ratio due to the decrease in water content is linearly related (line 1 in Fig. 3). This type of shrinkage is called normal shrinkage.

However, in structured and well-aggregated soils or soils with considerable biological activity, there are large inter-aggregate pores and biological tubular pores that are caused by worm and root channels (Cornelis et al., 2006). When these pores are emptied, there is a negligible change in the bulk volume as the air enters these relatively large pores (Cornelis et al., 2006) and causes the slope of the shrinkage curve to be as small as 0.1 (Braudeau et al., 1999) (curve 2 in Fig. 3). This behaviour is called structural shrinkage (Mitchell, 1992). The most challenging task in constructing the shrinkage curve is the measuring of the total volume of the soil specimen. The total volume can be measured using four methods, namely, the direct measurement method (ASTM D2435/D2435M, 2011; ASTM D4186 2006, 2006; ASTM D6836-02 2008, 2008; Berndt and Coughlan, 1976; Braudeau et al., 1999; BS 1377-2, 1990; Liu et al., 2012; Umezaki and Kawamura, 2013, Yule and Ritchie, 1980a, b), the volume displacement method (ASTM D427 2004, 2004; ASTM D4943-08 2008, 2008; Brasher et al., 1966; BS 1377-2, 1990; Johnston and Hill, 1944; Lauritzen, 1948;Lauritzen and Stewart, 1942; McIntyre and Stirk, 1954; Monnier et al., 1973; Sibley and Williams, 1989), the two non-mixing liquid method (Guillermo et al., 2001) and the gamma ray attenuation double-energy method (Adejumo and Balogun, 2012). A method is considered to be destructive when the soil specimen is altered or disturbed due to the test procedure. Table 1 summarizes the methods that can be used to calculate the total volume of the soil specimen. The direct measurement method was used in this paper.

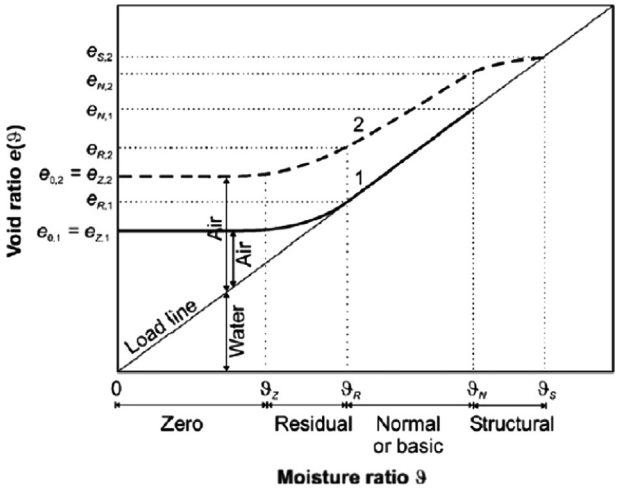

Fig. 3. Schematic representation of shrinkage curve of a non-structured soil (solid line 1) and a well-structured soil (dashed line 2) (from Cornelis et al., 2006).

A number of models have been proposed to describe the shrinkage curve (Fredlund et al., 2002; Giráldez and Sposito, 1983; Giráldez et al., 1983; Kim et al., 1992; Sposito and Giraldez, 1976); they are given in Cornelis et al. (2006).

The Fredlund et al. (2002) model, for the shrinkage curve used in this paper, has three curve-fitting parameters, namely, a_{sh}, b_{sh} and c_{sh}.

$$e(w) = a_{sh}\left[\frac{w^{C_{sh}}}{b_{sh}^{C_{sh}}} + 1\right]^{1/C_{sh}} \tag{1}$$

and

$$\frac{a_{sh}}{b_{sh}} = \frac{G_s}{S_0} \tag{2}$$

where e is the void ratio, w is the gravimetric water content, G_s is the specific gravity and S_0 is the initial degree of saturation. However, the curve-fitting parameters, a_{sh} and c_{sh}, can be related to the important properties of the shrinkage curve. The a_{sh} parameter is the minimum void ratio and the c_{sh} parameter is the curvature of the shrinkage curve. By rearranging Eq. (2), parameter b_{sh} can be expressed in terms of SL'

$$b_{sh} = \frac{a_{sh}S_0}{G_s} = SL' \tag{3}$$

where SL' is the apparent shrinkage limit that is dependent on the initial degree of saturation. At a water content of less than SL', there is a negligible change in the void ratio due to a further reduction in the water content. If the initial degree of saturation

Table 1
Methods to measure the void ratio during the shrinkage test.

Method	Destructive	Description
Direct measurement method	Non-destructive	Measurement devices, such as Vernier callipers, are used to obtain the dimensions of the specimen. It was assumed that the specimen had a regular geometry, such as a cylinder, so that the volume could be easily calculated. In order to account for the non-homogeneous geometry, several measurements were taken to obtain the average dimension. The simplicity, speed and non-destructiveness are the advantages of this method. This method may not work on irregular shaped specimens
Volume displacement method	Destructive	The soil specimen is coated with wax or saran resin dissolved in ethyl ketone (Brasher et al., 1966) and then submerged into the liquid. The volume of the liquid displaced equals the total volume of the specimen. It can be used to measure the volume of irregularly shaped specimens. The disadvantages of this method are that it is destructive and that when the clods have large pores, more viscous saran resins are needed (Guillermo et al., 2001)
Two non-mixing liquid method	Destructive	Two types of liquids are used to produce different buoyancy forces on the soil specimen. The difference in the buoyancy force is then used to calculate the density of the specimen, and hence, the total volume of the specimen. This method is similar to the volume displacement method
Gamma ray attenuation dual-energy method	Non-destructive	Dual energy gamma beams with different mass absorption coefficients are applied to obtain different mass attenuation coefficients and the numbers of gamma ray quanta produced, and hence, the bulk density and total volume. This method requires special apparatus and is the most expensive method compared to the others; however, it can be used to measure irregularly shaped specimens and it is not destructive

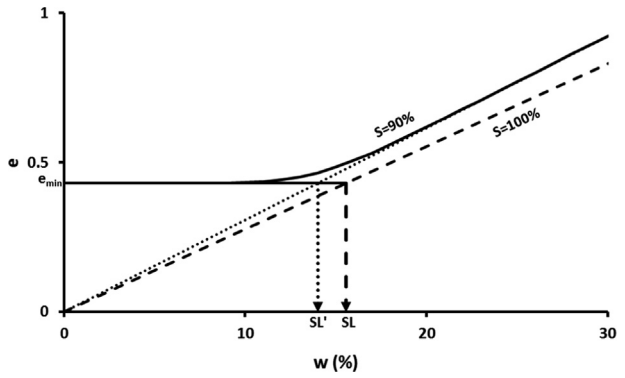

Fig. 4. Illustration of the effect of initial degree of saturation on shrinkage limit.

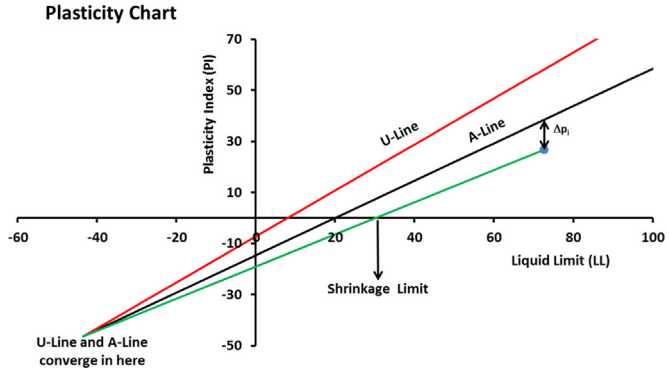

Fig. 5. Estimating shrinkage limit using plasticity chart.

during normal shrinkage is 100%, SL' equals SL. Fig. 4 describes how the initial degree of saturation affects the shrinkage limit.

Although there are three parameters, a_{sh}, b_{sh}, and c_{sh}, in Fredlund et al. (2002)'s model for the shrinkage curve, it is only necessary to estimate a_{sh} and c_{sh} as the ratio of a_{sh} and b_{sh} is fixed following Eq. (2).

The minimum void ratio can be estimated as the void ratio at shrinkage limit SL. The value of SL for fine-grained soils can be estimated using the plasticity chart shown in Fig. 5 (Casagrande, 1932). The A-line and the U-line are extended until they meet at coordinates (−43.5, −46.4). Connecting this meeting point with the data point plotted on the plasticity chart gives a line which intersects the liquid limit axis. The shrinkage limit is given by the intersection point, as shown in Fig. 5.

The accuracy of the above procedure in obtaining the shrinkage limit is comparable to the accuracy of the shrinkage limit test itself considering all of the problems and uncertainties in the test (Holtz et al., 2011). A comparison of the SL values obtained by the Casagrande method and the measured shrinkage limit was performed using Kayabali (2012) data.

Kayabali (2012) tested 100 soils from a lacustrine clay formation and compared the shrinkage limits obtained through the mercury method, the extrusion pressure method and the statistical method. The plastic and liquid limits, determined by ASTM D4318-10 (2010), were used to find the shrinkage limit using the Casagrande (1932) method. A comparison of the estimated shrinkage limit, from the Casagrande (1932) method,

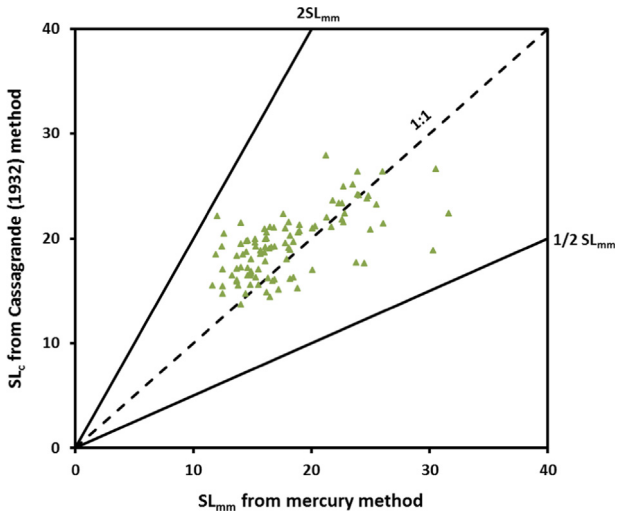

Fig. 6. Comparison of shrinkage-limit from Casagrande (1932) method and from mercury method (using data from Kayabali, 2012).

and the shrinkage limit, by ASTM D427 (2004), is shown in Fig. 6. The estimated SL values were mainly within half (50%) to two times (200%) of the SL from the ASTM D427 (2004), which shows that the estimation and the measurement of the shrinkage limit are equally inaccurate. A similar observation was made by Holtz et al. (2011).

The effects of varying a_{sh} and c_{sh} on the shrinkage curve and the SWCC-S are illustrated in Fig. 7. In Fig. 7, b_{sh} is calculated using Eq. (2) for each value of a_{sh}. Fig. 7e and f shows that a_{sh} is more significant in affecting the AEV compared to c_{sh}. As the effect of c_{sh} on the shrinkage curve is not significant, Fredlund et al. (2002) proposed values of $c_{sh}=9.57$, 25.31 and 8.47 for undisturbed soil, initially slurried soil and compacted soil, respectively.

3. SWCC-*S* constructed from SWCC-*w* and shrinkage curve

The Fredlund and Xing (1994) equation was used to fit the SWCC as it offers high flexibility in matching the SWCC data (Leong and Rahardjo, 1997). The Fredlund and Xing (1994) equation was developed for the volumetric water content (θ), but can be re-written for the gravimetric water content (w), as shown below:

$$w = w_s \left\{ \frac{1}{\ln\left[\exp(1)+\left(\Psi/a\right)^n\right]} \right\}^m \frac{\ln\left[1+(\Psi/\Psi_r)\right]}{\ln\left[1+(1000000/\Psi_r)\right]} \quad (4)$$

where a, n, m and Ψ_r are curve-fitting parameters, w_s is the saturated gravimetric water content and Ψ is the matric suction. However, the curve-fitting parameters in the Fredlund and Xing (1994) equation are non-unique and are dependent on the initially assumed values. The parameters show relatively large variations when the SWCC data do not cover the entire matric suction region for SWCC (Leong and Rahardjo, 1997). Chin et al. (2010) devised the one-point method to estimate the Fredlund and Xing parameters by only using one pair of w and Ψ data (Chin et al., 2010). The estimations of the Fredlund and

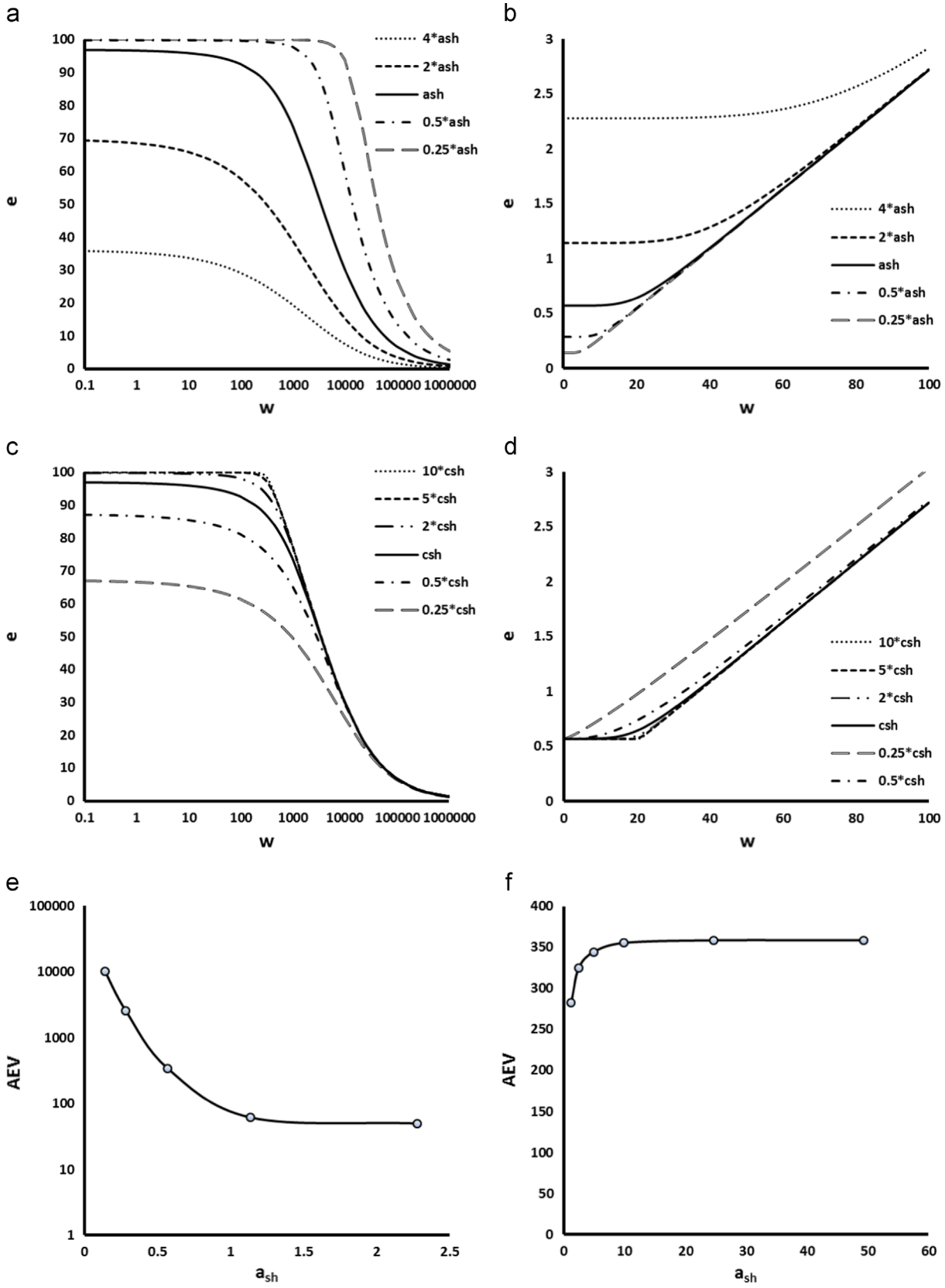

Fig. 7. Effect of varying a_{sh} and c_{sh} on shrinkage curve, SWCC-*S*, and AEV. (a) Effect of changing a_{sh} towards SWCC-S, (b) Effect of changing a_{sh} towards shrinkage curve, (c) Effect of changing c_{sh} towards SWCC-S, (d) Effect of changing c_{sh} towards shrinkage curve, (e) Effect of changing a_{sh} towards AEV, and (f) Effect of changing c_{sh} towards AEV.

Xing (1994) parameters for fine-grained soils are given as follows:

$$a_c = -2.4\chi + 722 \tag{5}$$

$$n_c = 0.07\chi^{0.4} \tag{6}$$

$$m_c = 0.015\chi^{0.7} \tag{7}$$

$$\Psi_{rc} = |914\exp(-0.002\chi)| \tag{8}$$

where χ is a curve-fitting parameter that relates all of the curve-fitting parameters in the Fredlund and Xing (1994) equation. Parameter χ in the Chin et al. (2010) method is used to adjust the SWCC to be on the selected pair of SWCC data. Chin et al. (2010) defined fine-grained soils as soils with a percentage finer than 200 μm being greater than or equal to 30%. All the soils used in this study are fine-grained soils by following Chin et al. (2010)'s definition. Chin et al. (2010) showed that by using the water content at a matric suction of either 100 or 500 kPa, gives equally good estimates for the SWCC of fine-grained soils. In this study, the Chin et al. (2010) method was used to obtain the initial estimates of the Fredlund and Xing (1994) parameters of a_f, n_f, m_f and Ψ_r. Afterwards, curve fitting was performed to minimise the error between the SWCC-w data and the Fredlund and Xing (1994) equation. This procedure served two purposes: (1) the parameters obtained were more consistent as the initial estimates were obtained from close estimates, and (2) the curve fitting provided a consistent treatment for cases with incomplete SWCC-w data where the SWCC-w data were missing at high suction values.

For some of the SWCC-w data, the "soil" was initially in slurry form and the initial water content could be much higher than the liquid limit. In a strict sense, slurry is not a soil. At the liquid limit, the soil particles are hardly in contact as the soil behaves as a liquid. For such a SWCC, it is proposed that the liquid limit shall be taken as the initial water content of the soil, w_s, if the initial water content is greater than the liquid limit. An example is shown in Fig. 8.

The SWCC-w and the shrinkage curve can be combined using the following phase relationship:

$$S(\Psi) = \frac{w(\Psi) \times G_s}{e(w)} \tag{9}$$

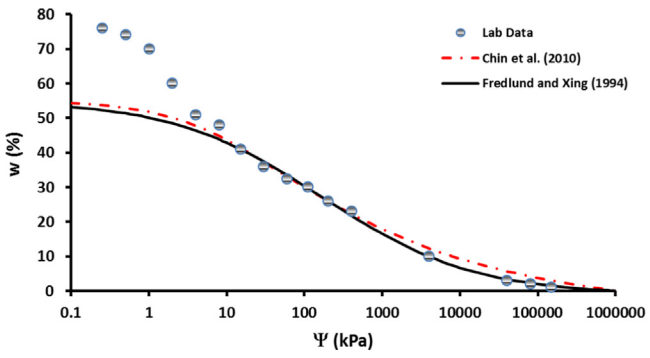

Fig. 8. A fitted SWCC-w for Box2-0.1SFR soil from Fredlund et al. (2011) with w_s taken as liquid limit.

where S is the degree of saturation, w is the gravimetric water content, G_s is the specific gravity and e is the void ratio.

4. Determination of AEV

Zhai and Rahardjo (2012) proposed determining the AEV by using a mathematical method thus giving more consistent AEV values. Based on Zhai and Rahardjo (2012), the AEV of the SWCC can be obtained from the intersection point between the initial horizontal line and the tangent line at the inflection point. The intersection point is given by

$$\text{AEV} = \Psi_i 10^{(S_0 - S_i)/m_i} \tag{10}$$

and

$$m_i = \frac{S_i - S_0}{\log(\Psi_i/\text{AEV})} \tag{11}$$

where m_i is the slope of the inflection point, S_i is the degree of saturation at the inflection point, S_0 is the initial degree of saturation and Ψ_I is the matric suction at the inflection point.

However, the equation in Zhai and Rahardjo (2012) requires the SWCC-S to be curve fitted with the Fredlund and Xing (1994) equation. A simpler method is hereby suggested to obtain the slope at inflection point m_i by calculating the slope of the SWCC-S, m_s for piecewise segments, namely,

$$m_s = \frac{S(\Psi) - S(\Psi - \Delta\Psi)}{\log(\Psi/(\Psi - \Delta\Psi))} \tag{12}$$

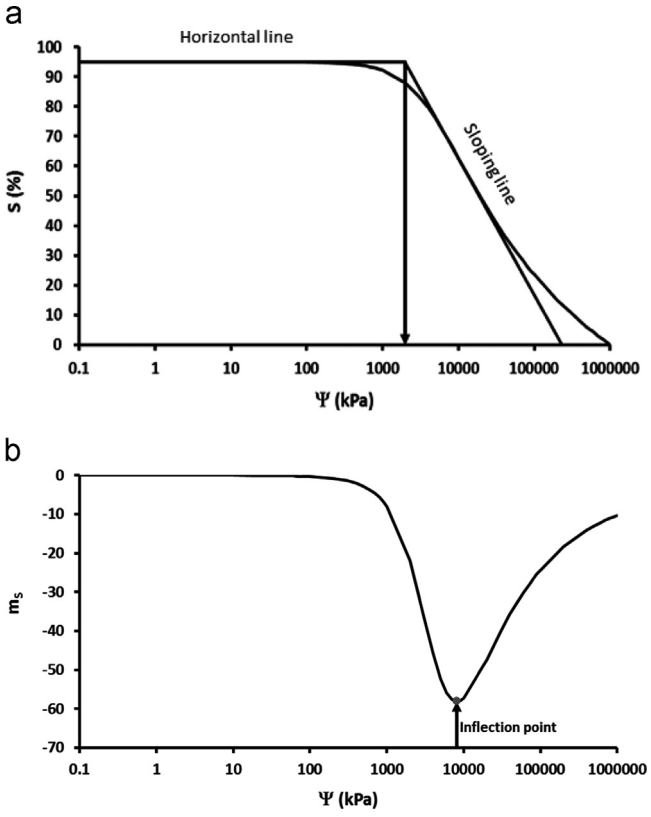

Fig. 9. SWCC-S and m_s of Regina clay (data from Fredlund, 1964). (a) SWCC-S and (b) m_s.

where $S(\Psi)$ is calculated from Eq. (9) and $\Delta\Psi$ is the small change in suction. The results of calculating m_s with Eq. (11) for the entire SWCC-S are given in Fig. 9b. The value of m_i is given by the minimum slope (m_s) of the SWCC-S, as indicated in Fig. 9b for Regina clay.

5. Sensitivity analyses of the shrinkage curve parameters on AEV of the soils

In this paper, shrinkage curve parameters a_{sh}, b_{sh} and c_{sh} were obtained by curve fitting the shrinkage curve, while the AEVs of the soils were obtained with Eqs. (10) and (12). Data on forty types of soil were collated from the SoilVision (2003) database and the literature (Fleureau et al., 2002; Fredlund, 1964; Kong and Tan, 2000; Krisdani et al., 2008; Peron et al., 2007; Zhan et al., 2007). The criteria for selecting these forty soils were that they must have:

1. SWCC-w,
2. Either shrinkage curve, SWCC-θ or SWCC-S, and
3. Basic soil properties (G_s, PL, LL and w_0).

The basic properties and shrinkage curve parameters a_{sh}, b_{sh} and c_{sh} of the 40 soils are shown in Table 2, while their SWCC-w curve-fitting parameters are given in Table 3.

Table 2
Basic properties of 40 soils.

S/N	Soil Counter	Reference	G_s	PL (%)	LL (%)	PI (%)	SL (%)	W_s (%)	Fredlund et al. (2002)		
									a_{sh}	b_{sh}	c_{sh}
1	Box2-0.1SFR	Fredlund et al. (2011)	2.50	30	55	25	20	55.0	0.350	0.140	20.24
2	Box5-0.1SFR	Fredlund et al. (2011)	2.50	30	55	25	20	47.0	0.350	0.140	20.24
3	Box6-0.8SFR	Fredlund et al. (2011)	2.50	15	38	23	12	25.0	0.360	0.140	25.34
4	Box11-0.8SFR	Fredlund et al. (2011)	2.50	15	38	23	12	38.0	0.350	0.140	20.24
5	RS100 (Sandy silt-ML) 100% Residual soil	Krisdani et al. (2008)[a]	2.65	32	47	15	25	47.0	0.870	0.330	4.66
6	MRF80–20 (Sandy silt-ML) 80% Residual soil+20% fine sand	Krisdani et al. (2008)[a]	2.65	27	41	14	21	41.0	0.830	0.310	3.142
7	MRF60–40 (Silty sand-SM) 60% Residual soil+40% fine sand	Krisdani et al. (2008)[a]	2.65	22	34	12	18	34.0	0.699	0.260	4.315
8	Saturated slurry of Jossigny silt (Jossigny loam)	Fleureau et al. (2002)	2.74	16	37	21	12	37.0	0.430	0.160	8.235
9	FoCa Clay	Fleureau et al. (2002)	2.68	35	90	55	18	90.0	0.300	0.110	19.13
10	LaVerne Clay-Slurry	Fleureau et al. (2002)	2.71	19	35	16	15	35.0	0.780	0.290	8.69
11	LaVerne Clay-Compacted	Fleureau et al. (2002)	2.71	18	35	17	14	32.0	0.780	0.290	17.59
12	12398	SoilVision (2003)	2.67	26	78	52	14	33.2	0.468	0.180	10.55
13	12400	SoilVision (2003)	2.65	24	60	36	15	31.6	0.583	0.220	7.076
14	12425	SoilVision (2003)	2.72	27	40	13	22	30.3	0.573	0.210	5.314
15	12428	SoilVision (2003)	2.7	24	71	47	13	31.6	0.418	0.150	4.355
16	12430	SoilVision (2003)	2.73	16	51	35	10	21.0	0.367	0.130	6.009
17	12431	SoilVision (2003)	2.83	33	85	52	17	48.3	0.551	0.190	3.602
18	12432	SoilVision (2003)	2.69	24	71	47	13	71.0	0.417	0.160	4.102
19	12433	SoilVision (2003)	2.8	26	92	66	12	92.0	0.461	0.160	2.739
20	12434	SoilVision (2003)	2.73	16	51	35	10	51.0	0.367	0.130	6.009
21	12435	SoilVision (2003)	2.83	33	85	52	17	85.0	0.551	0.190	5.461
22	12436	SoilVision (2003)	2.73	31	64	33	19	64.0	0.577	0.210	3.436
23	12445	SoilVision (2003)	2.61	32	64	32	20	40.6	0.837	0.320	92.16
24	12446	SoilVision (2003)	2.61	29	53	24	20	33.7	0.660	0.250	40.7
25	12499	SoilVision (2003)	2.61	32	64	32	20	39.7	0.835	0.320	18.22
26	12442	SoilVision (2003)	2.84	38	70	32	24	70.0	0.379	0.130	4.445
27	12447	SoilVision (2003)	2.61	32	64	32	20	36.1	0.719	0.280	23.42
28	12448	SoilVision (2003)	2.72	17	36	19	13	21.5	0.513	0.190	24.74
29	WTP-2	NTU[b]	2.60	28	47	19	21	27.0	0.627	0.240	22.98
30	WTP 3	NTU[b]	2.50	28	47	19	21	25.5	0.590	0.240	10.54
31	WTP 1	NTU[b]	2.55	28	47	19	21	27.7	0.630	0.250	100.0
32	WTP 4	NTU[b]	2.50	28	47	19	21	25.1	0.570	0.230	18.89
33	Clayey silt from Bioley	Peron et al. (2007)	2.75	16.9	31.8	14.9	13	31.8	0.583	0.210	47.58
34	Silty clay	Kong and Tan (2000)	2.77	34.7	81.7	47	19	45.0	0.431	0.140	4.589
35	Regina clay-initially slurried	Fredlund (1964)	2.83	24.9	75.5	50.6	13	75.5	0.489	0.160	4.199
36	Regina clay-pc 25 kPa	Fredlund (1964)	2.83	24.9	75.5	50.6	13	72.0	0.489	0.160	4.199
37	Regina clay-pc 400 kPa	Fredlund (1964)	2.83	24.9	75.5	50.6	13	51.0	0.489	0.160	4.199
38	12402	SoilVision (2003)	2.67	26	78	52	14	48.3	0.600	0.220	7.294
39	Brownish-yellow expansive clay	Zhan et al. (2007)	2.67	19.5	50.5	31	13	30.5	0.507	0.190	20.15
40	Expansive clay from Karnataka state	Thyagaraj and Rao (2010)	2.71	23	82	59	12	64.7	1.286	0.470	11.08

[a]SWCC-w is calculated from SWCC-S and shrinkage curve.
[b]Nanyang Technological University, Singapore.

The ranges in a_{sh}, b_{sh} and c_{sh} were from 0.3 to 1.287, 0.112 to 0.475 and 2.74 to 92.16, respectively.

Sensitivity analyses were performed to investigate the effect of the shrinkage curve parameters, a_{sh} and c_{sh}, on the determination of the AEV. It is not necessary to investigate b_{sh} as parameters a_{sh} and b_{sh} are related by Eq. (2). The sensitivity analyses were performed in the following two ways:

1. Maintaining a constant c_{sh} and varying the a_{sh} parameter (and hence, b_{sh}) in the shrinkage curve equation (Eq. (1)), and
2. Maintaining a constant a_{sh} (and hence, b_{sh}) and varying the c_{sh} parameter in the shrinkage curve equation (Eq. (1)).

In order to carry out the first sensitivity analysis, it is necessary to know the probable errors that cause the variation in a_{sh}. Considering that the easiest way to estimate a_{sh} is to use the shrinkage limit, the accuracy of a_{sh} will therefore also be dependent on the accuracy of the shrinkage limit determination. The effect of the error in estimating the shrinkage limit on the estimation of a_{sh} is examined below.

A small change in the void ratio, δe, due to a small change in the water content, δw, is obtained as follows:

$$\frac{\delta e}{\delta w} = \frac{de(w)}{dw} = a_{sh}\left[\frac{w^{C_{sh}}}{b_{sh}^{C_{sh}}}+1\right]^{(1/csh)-1}\frac{w^{C_{sh}-1}}{b_{sh}^{C_{sh}}} \tag{13}$$

Therefore, the small error in void ratio $\delta e(w)$ is given as

$$\delta e(w) = \frac{a_{sh}\left[(w^{C_{sh}}/b_{sh}^{C_{sh}})+1\right]^{1/csh}}{\left[(w^{C_{sh}}/b_{sh}^{C_{sh}})+1\right]}\frac{w^{C_{sh}}}{b_{sh}^{C_{sh}}}\frac{\delta w}{w} \tag{14}$$

Table 3
SWCC curve-fitting parameters for 40 soils.

S/N	Chin et al. (2010))						Fredlund and Xing (1994)				
	a_c (kPa)	n_c	m_c	Ψ_{rc} (kPa)	χ	R^2	a (kPa)	n	m	Ψ_r (kPa)	R^2
1	9.13	0.68	0.81	504.61	297.03	0.987	63.98	0.46	1.84	1657.54	0.987
2	21.27	0.68	0.80	509.73	291.97	0.988	45.12	0.77	0.99	845.74	0.994
3	49.41	0.67	0.78	521.83	280.25	0.983	83.82	0.84	1.00	310.01	0.989
4	1.88	0.69	0.81	501.57	300.05	0.886	9.25	1.20	0.75	248.73	0.992
5	7.16	0.68	0.81	503.78	297.85	0.951	4.96	1.58	0.45	692.87	0.993
6	9.87	0.68	0.81	504.91	296.72	0.949	6.24	0.62	0.80	571.50	0.952
7	16.96	0.68	0.80	507.91	293.77	0.981	12.24	0.63	0.79	650.08	0.990
8	77.95	0.66	0.75	534.39	268.35	0.995	49.63	0.57	0.67	291.18	0.998
9	35.83	0.67	0.79	515.96	285.90	0.963	13.84	0.88	0.38	103.39	0.990
10	16.46	0.68	0.80	507.70	293.97	0.968	15.23	0.61	0.83	514.81	0.970
11	1.11	0.69	0.81	501.24	300.37	0.957	2.52	1.88	0.53	965.67	0.988
12	228.55	0.59	0.62	605.84	205.60	0.998	281.48	0.59	0.85	3570.17	0.999
13	184.08	0.61	0.66	583.81	224.13	0.990	69.65	0.64	0.47	1096.41	0.997
14	158.55	0.62	0.68	571.52	234.77	0.984	659.11	0.52	1.87	1773.23	0.997
15	405.70	0.49	0.46	702.22	131.79	0.996	1301.82	0.47	0.91	1721.23	0.998
16	335.57	0.53	0.53	662.36	161.01	0.970	218.20	0.60	0.12	247.73	0.996
17	347.25	0.53	0.51	668.84	156.15	0.993	880.79	0.68	0.85	1279.06	0.998
18	18.99	0.68	0.80	508.76	292.92	0.992	16.98	0.60	0.86	646.11	0.991
19	5.38	0.68	0.81	503.03	298.59	0.981	8.46	1.43	0.57	1520.34	0.999
20	12.53	0.68	0.80	506.03	295.61	0.987	7.91	1.55	0.41	401.85	0.999
21	32.75	0.67	0.79	514.63	287.19	0.994	32.18	0.64	0.77	522.73	0.994
22	47.87	0.67	0.78	521.16	280.89	0.991	29.27	0.64	0.60	273.58	0.996
23	165.46	0.62	0.68	574.82	231.89	0.441	1487.52	5.99	0.92	5382.79	0.938
24	77.82	0.66	0.75	534.33	268.41	0.260	1242.72	3.71	0.87	1242.72	0.922
25	149.98	0.63	0.69	567.45	238.34	0.281	1015.42	6.23	0.79	1015.42	0.921
26	359.62	0.52	0.50	675.77	150.99	0.951	220.45	0.04	0.06	220.45	0.994
27	82.08	0.65	0.75	536.23	266.63	0.257	1252.11	7.64	0.59	1252.11	0.925
28	372.28	0.51	0.49	682.94	145.72	0.382	1065.47	3.50	1.14	1065.47	0.979
29	539.08	0.40	0.31	784.78	76.22	0.670	539.08	0.40	0.31	784.78	0.670
30	613.38	0.32	0.22	834.90	45.26	0.511	1315.88	0.30	0.38	3694.75	0.778
31	393.65	0.50	0.47	695.20	136.81	0.862	431.01	0.64	0.37	723.94	0.953
32	559.88	0.38	0.29	798.50	67.55	0.938	2065.68	0.48	0.80	4667.25	0.950
33	53.88	0.67	0.77	523.78	278.38	0.892	26.76	1.67	0.34	1747.39	0.975
34	7.86	0.68	0.81	504.07	297.56	0.437	10.32	3.77	0.97	2592.40	0.995
35	18.28	0.68	0.80	508.47	293.22	0.914	68.99	0.96	0.85	362.13	0.998
36	23.43	0.68	0.80	510.65	291.07	0.939	82.51	1.00	0.89	836.60	0.997
37	128.15	0.63	0.71	557.22	247.44	0.969	480.21	0.73	1.29	702.06	0.993
38	235.66	0.59	0.62	609.44	202.64	0.986	202.94	0.55	0.59	576.86	0.987
39	304.00	0.55	0.56	645.16	174.17	0.830	332.09	0.35	0.72	1189.16	0.989
40	300.95	0.55	0.56	643.52	175.44	0.829	277.20	1.74	0.44	404.01	0.973

Dividing Eq. (14) by Eq. (1) gives

$$\delta e(w) = \frac{e(w)}{\left[(w^{C_{sh}}/b_{sh}^{C_{sh}})+1\right]} \frac{w^{C_{sh}}}{b_{sh}^{C_{sh}}} \frac{\delta w}{w} \tag{15}$$

Eq. (15) can be simplified for the case where $e = e_{min}$ and theoretically $w \approx SL'$:

$$\delta e(w) = e_{min} \frac{1}{\left[\frac{SL'^{C_{sh}}}{SL'^{C_{sh}}}+1\right]} \frac{SL'^{C_{sh}}}{SL'^{C_{sh}}} \frac{\delta w}{SL'} \tag{16}$$

or

$$\delta e(w) = e_{min} \frac{1}{[1+1]} 1 \frac{\delta w}{SL'} = 0.5 e_{min} \frac{\delta w}{SL'} \tag{17}$$

Based on Fig. 6, the estimation of the shrinkage limit might have an error of δw up to 100%. Therefore, taking an extreme case, in which the error is 100%, Eq. (17) will decrease to

$$\delta e(w) = 0.5 e_{min} \tag{18}$$

Considering that the error in e_{min}, due to the estimation in the shrinkage limit, can be up to $0.5e_{min}$, the sensitivity analysis was performed using three a_{sh} values, namely, $SL.G_s$, a_{sh} equals $e_{min}+0.5e_{min}$ (or $1.5e_{min}$) and $e_{min}-0.5e_{min}$ (or $0.5e_{min}$). The effect of a_{sh} on the AEV is shown in Fig. 10. In

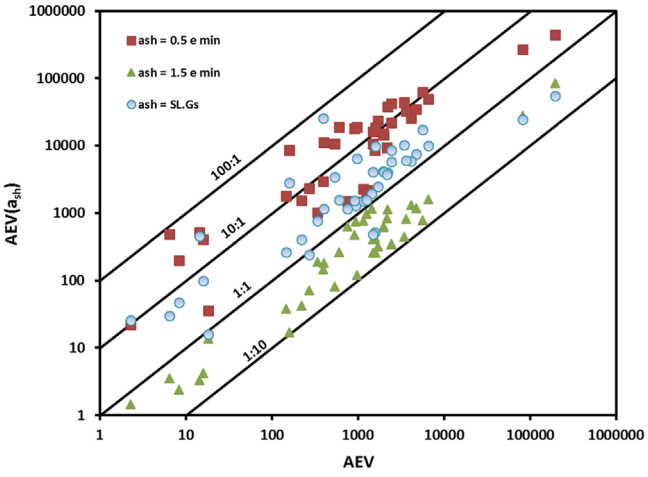

Fig. 10. Effect of a_{sh} on AEV for the 40 soils.

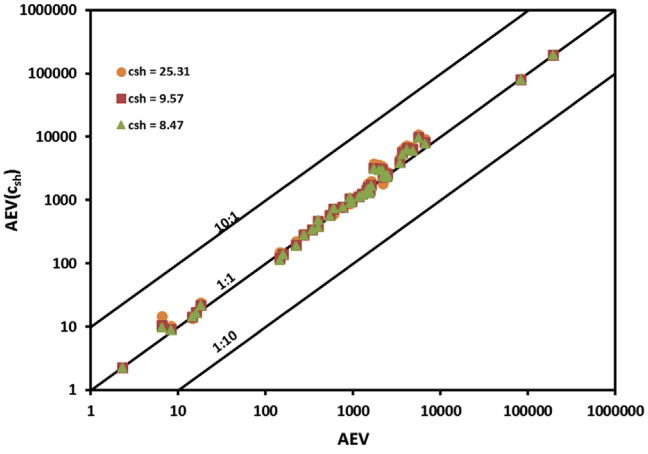

Fig. 11. Effect of c_{sh} on AEV for the 40 soils.

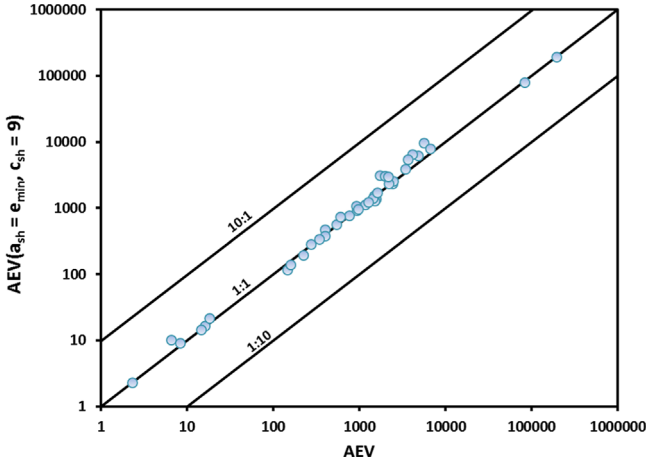

Fig. 12. Estimation of AEV assuming $c_{sh}=9$ for the 40 soils.

Fig. 10, AEV is the measured value, while AEV(a_{sh}) is the AEV that is obtained by varying a_{sh}.

For the second sensitivity analysis, three different c_{sh} values were used. The three values for c_{sh} were recommended by Fredlund et al. (2002); they are 9.57, 25.31 and 8.47 for undisturbed soil, initially slurried soil and compacted soil, respectively. Therefore, these three c_{sh} values were used in the sensitivity analysis. The effect of c_{sh} on the AEV for the 40 soils is shown in Fig. 11. In Fig. 11, AEV (c_{sh}) is the AEV that is obtained by varying c_{sh}.

Based on the sensitivity analyses, a_{sh} is a very important parameter in affecting the AEV. The error in determining the AEV, due to an error in determining a_{sh}, can be up to 100 times the actual AEV in very extreme cases (Fig. 10). On the other hand, c_{sh} does not seem to have a significant effect on the determination of the AEV (Fig. 11). Most of the soils encountered in engineering practice are either compacted or in the in-situ (undisturbed) condition. Therefore, a typical c_{sh} of 9 (average c_{sh} values for compacted and undisturbed conditions) is recommended. Fig. 12 shows a comparison between the actual AEV and the AEV estimated with a c_{sh} equal to 9. It shows that there is no significant difference between the actual AEV and the AEV estimated with a c_{sh} equal to 9.

6. Error in estimating minimum void ratio

Based on the sensitivity analyses, it is not possible to attain high accuracy for AEV unless minimum void ratio e_{min}, i.e., a_{sh}, is known. The errors in measuring e_{min} depend on the measurement devices and can be evaluated mathematically as follows.

Void ratio is the ratio of the volume of voids V_v to the volume of solid V_s, namely,

$$e = \frac{V_v}{V_s} = \frac{V_t}{V_s} - 1 \tag{19}$$

$$V_s = \frac{M_t}{G_s \times \rho_w} \frac{1}{1+w} \tag{20}$$

Since V_s can be obtained using total mass M_t, water content w and specific gravity G_s (whose measurement is based on weight), the error in measuring V_s can be very small, and

therefore, can be ignored. However, the total volume is calculated by measuring the dimensions of the soil specimen (in the case of a cylindrical specimen, the radius, r, and the height, h); and therefore, the error in measuring the total volume depends on the accuracy of the measuring instruments. In the case of Vernier callipers, the accuracy is ± 0.1 mm. Hence, the error in estimating the void ratio (δe), due to the error in measuring the radius (δr) and the height (δh) of a cylindrical soil specimen, can be written as

$$\delta e = \frac{1}{Vs}\left(2\pi rh\delta r + \pi r^2\delta h\right) = \frac{\pi r^2 h}{V_s}\left(2\frac{\delta r}{r} + \frac{\delta h}{h}\right) = \frac{V_t}{V_s}\left(2\frac{\delta r}{r} + \frac{\delta h}{h}\right) \quad (21)$$

or

$$\delta e = \left(2\frac{\delta r}{r} + \frac{\delta h}{h}\right)(1 + e_{\min}) \quad (22)$$

Since δr and δh depend on the accuracy of Vernier callipers, $\delta r = \delta h$ and Eq. (22) can be simplified to

$$\delta e = \delta r\left(\frac{2}{r} + \frac{1}{h}\right)(1 + e_{\min}) = f(\delta r, r, h)(1 + e_{\min}) \quad (23)$$

where

$$f(\delta r, r, h) = \delta r\left(\frac{2}{r} + \frac{1}{h}\right) \quad (24)$$

For a soil specimen with a radius of 25 mm, the values for f (δr, r and h) are given in Fig. 13.

Based on Fig. 13, $f(\delta r,r,h)$ equals 0.018 for an h equal to 10 mm. For larger h values, it will converge to 0.01. Therefore, for $h = 10$ mm and $r = 25$ mm, $f(\delta r,r,h)$ equals 0.02. Substituting this value into Eq. (23), δe can be obtained as

$$\delta e = 0.02(1 + e_{\min}) = 0.02 + 0.02e_{\min} \quad (25)$$

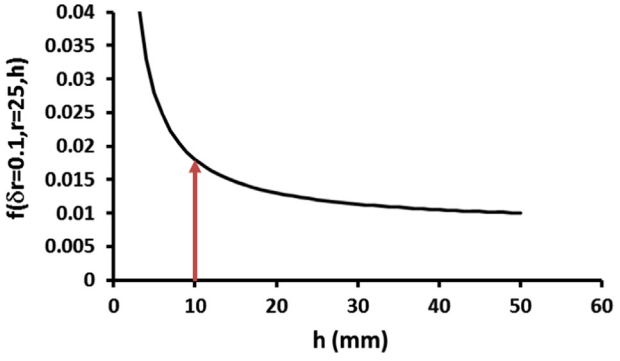

Fig. 13. Values of $f(\delta r = 0.1, r = 25, h)$ values for different heights h of soil specimens.

The error in a_{sh} from using SL is $0.5e_{\min}$, whereas the error in a_{sh} from measurements of the final dimensions of the soil specimen on the drying path is $(0.02e_{\min} + 0.02)$. Using the smallest $e_{\min}$ ($=0.3$) from the database of 40 soils, it can be seen that δe using SL is about 0.15, while δe due to measurement of the soil specimen volume is 0.008. Therefore, it is recommended that $e_{\min}$, i.e., a_{sh}, be determined from the direct measurement of the volume of the soil specimen.

7. Variation in AEV of a kaolin specimen due to the measurement inaccuracy

Shrinkage tests were carried out to construct the shrinkage curve using unrestrained cylindrical kaolin specimens under different drying conditions. Kaolin slurry was made by mixing kaolin powder at a water content of about 1.5 times the liquid limit. The slurry was placed into a consolidation tank, 30 cm in diameter, and then consolidated one-dimensionally under a pressure of 150 kPa. At the end of consolidation, the kaolin sample was extruded and then cut using a ring (height of 1.9 cm and diameter of 6.3 cm) with a sharp edge. The basic soil properties of the kaolin specimens are given in Table 4.

Five kaolin specimens were prepared using this procedure. Specimens 1 and 2 were dried in the open air (laboratory environment: relative humidity ranges from 60 to 70%), while specimen 3 was placed inside a desiccator containing a salt solution with a relative humidity of 82%. Specimen 4 was placed inside a pressure plate apparatus and then slowly dried by increasing the air pressure while maintaining water pressure at the atmospheric pressure. Specimen 5 was dried in the oven. However, drying specimen 5 in the oven caused the specimen to crack; and therefore, its volume could not be measured and its volume was not reported in this paper. The dimensions of the specimens were measured each time the weights of the specimens were measured. Four readings of height and diameter were taken following the ASTM standard (ASTM D2435/D2435M, 2011, ASTM D6836-02 2008, 2008, ASTM D4186 2006, 2006).

Changes in weight and void ratio of the specimens dried in the open air (specimens 1 and 2) and in the desiccator with the salt solution (specimen 3) are shown in Figs. 14 and 15, respectively. Based on Fig. 14, the kaolin specimens (specimen 1 and 2) dried in the open air required up to two days to reach the minimum void ratio and three days to completely dry the soils. The kaolin specimen (specimen 3) that was placed inside the desiccator (Fig. 15) required up to five days for the specimen to reach the minimum void ratio and 25 days to completely dry the specimen. However, the kaolin specimens that were dried in the open air have the same minimum void ratio as the kaolin specimen that was placed inside the

Table 4
Basic properties of the kaolin specimens.

S (%)	e	w (%)	θ (m^3/m^3)	ρ_{dry} (t/m^3)	ρ_t (t/m^3)	γ_t (kN/m^3)	G_s	PL (%)	LL (%)	PI (%)	SL (%)
98.01	1.63	60	60.75	1.01	1.62	15.86	2.66	46	72	26	30

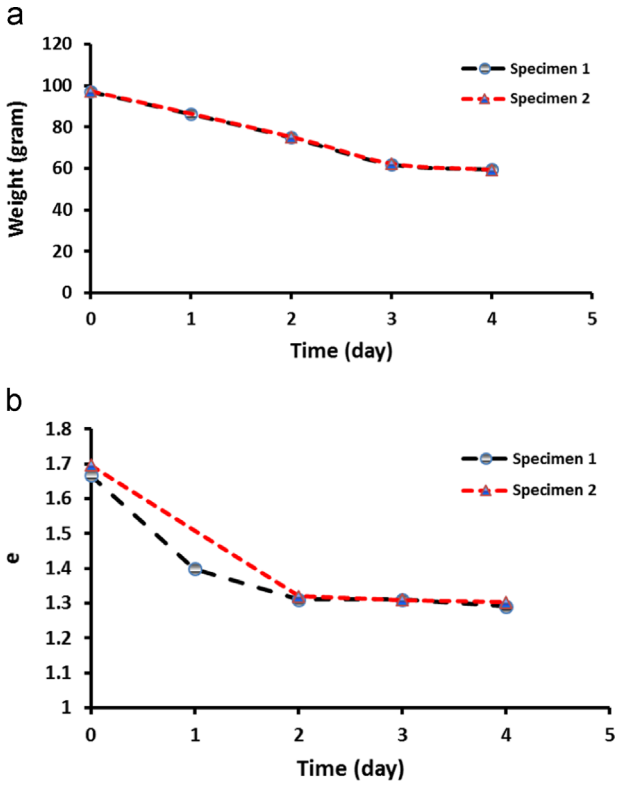

Fig. 14. Measurement of weight and void ratio of kaolin specimen drying in the open air. (a) Weight change and (b) Void ratio change.

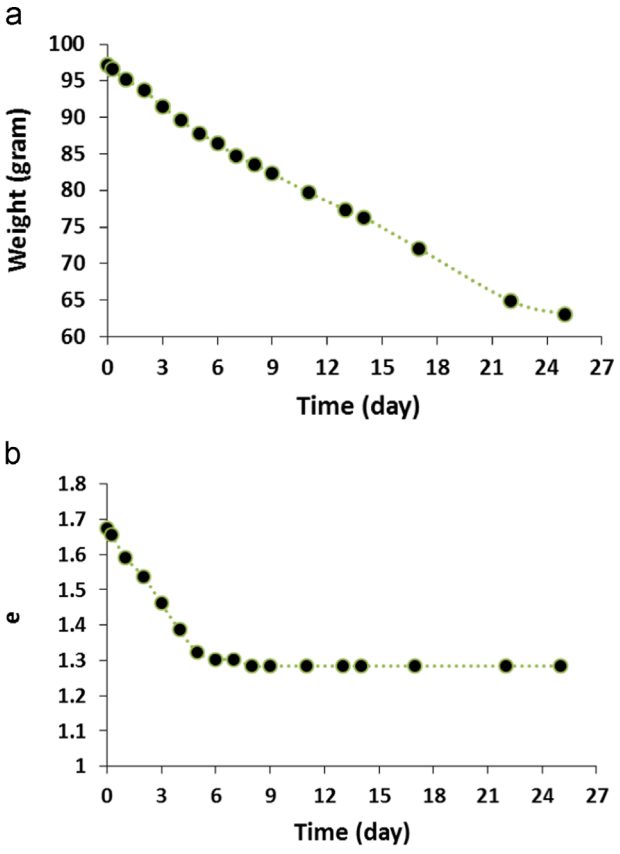

Fig. 15. Measurement of weight and void ratio of kaolin specimen drying in the desiccator with salt solution. (a) Weight change and (b) Void ratio change.

desiccator. Therefore, drying the soil specimen in open air was sufficient for obtaining the minimum void ratio (a_{sh}). The shrinkage curve estimated by using $c_{sh}=9$ and the measured minimum void ratio ($e_{min}=1.289$) is plotted with the shrinkage data for the three kaolin specimens in Fig. 16. The b_{sh} value was calculated to be 47.5% from Eq. (2). It can be seen that there is good agreement between the shrinkage curve and the shrinkage data. Specimen 4 was used to construct the SWCC-w, as shown in Fig. 17a. Combining the shrinkage curve from Fig. 16 and the SWCC-w from Fig. 17a, the SWCC-S is constructed as shown in Fig. 17b. Based on Fig. 17b, the AEV of the kaolin specimen was determined at 340 kPa.

By assuming that the shrinkage is homogeneous, i.e., that the shape of the specimen remains uniform, the variation in void ratio can be calculated using Eq. (23) such that

$$\delta e=\delta r\left(\frac{2}{r}+\frac{1}{h}\right)(1+e_{min})=0.1\left(\frac{2}{31.5}+\frac{1}{19}\right)(1+1.289)=0.027 \quad (26)$$

Therefore, e_{min} for the kaolin specimen can range from 1.262 to 1.316. The AEVs for the two void ratios are 356 kPa and 325.68 kPa, respectively.

A significant difference (17%) was found between SL' and SL (47.5% and 30.5%). Therefore, assuming that the error in determining the shrinkage limit, δw, can be $\pm 17\%$, the error in estimating the minimum void ratio is given as follows:

$$\delta e(w)=0.5e_{min}\frac{\delta w}{SL'}=0.5(1.289)\frac{\pm 17}{30.5}=\pm 0.36 \quad (27)$$

Thus, the e_{min} calculated with the shrinkage limit in this case will range from 0.929 to 1.649. The AEVs that are calculated using these values are 624.9 kPa and 212.8 kPa, respectively. Fig. 18a shows the ratio of AEV ($a_{sh}=e_{min}\pm\delta e$) and AEV ($a_{sh}=e_{min}$) for the kaolin specimens versus a_{sh}, while Fig. 18b shows the value of AEV with respect to different a_{sh}. Fig. 18 shows that the error in determining the AEV using the measured e_{min} as a_{sh} is much smaller than the error using a_{sh} estimated from the shrinkage limit.

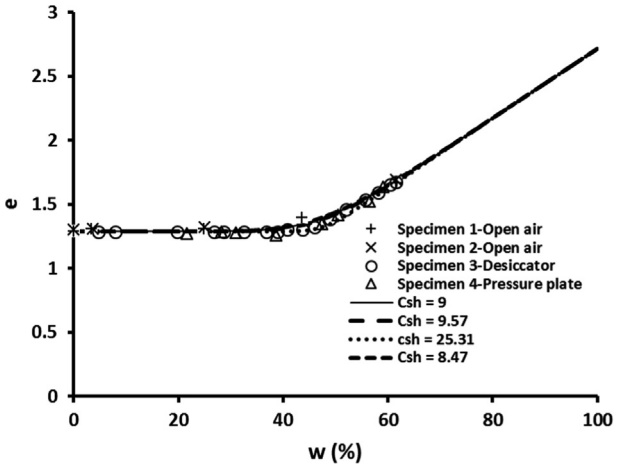

Fig. 16. Shrinkage curve of the kaolin specimen.

The goodness of fit of the estimated shrinkage curve (Eq. (1)) using $a_{sh}=e_{min}$ and $c_{sh}=9$ was further verified with the data of Cornelis et al. (2006). Cornelis et al. (2006)

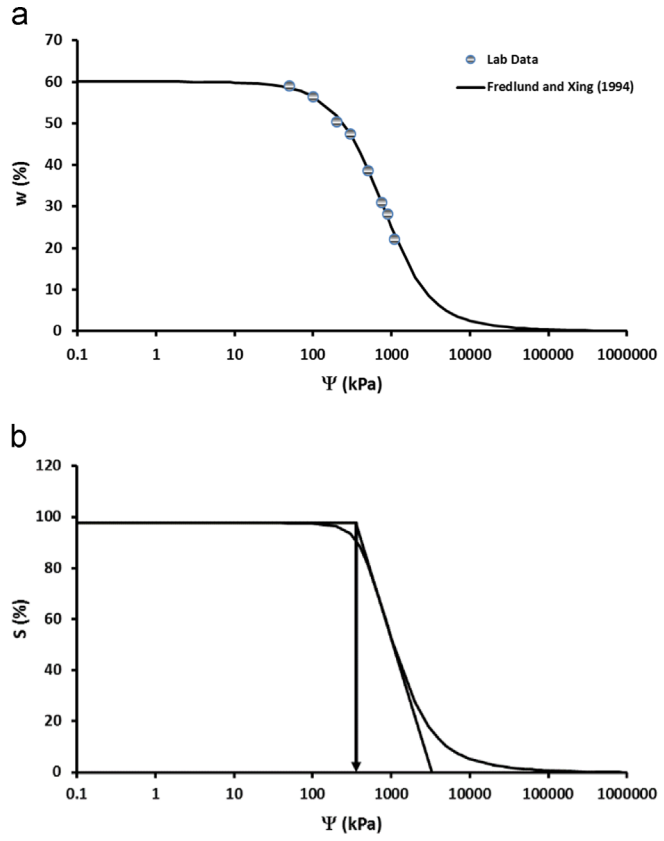

Fig. 17. SWCC of the kaolin specimens. (a) SWCC-w of the kaolin specimens and (b) SWCC-S of the kaolin specimens.

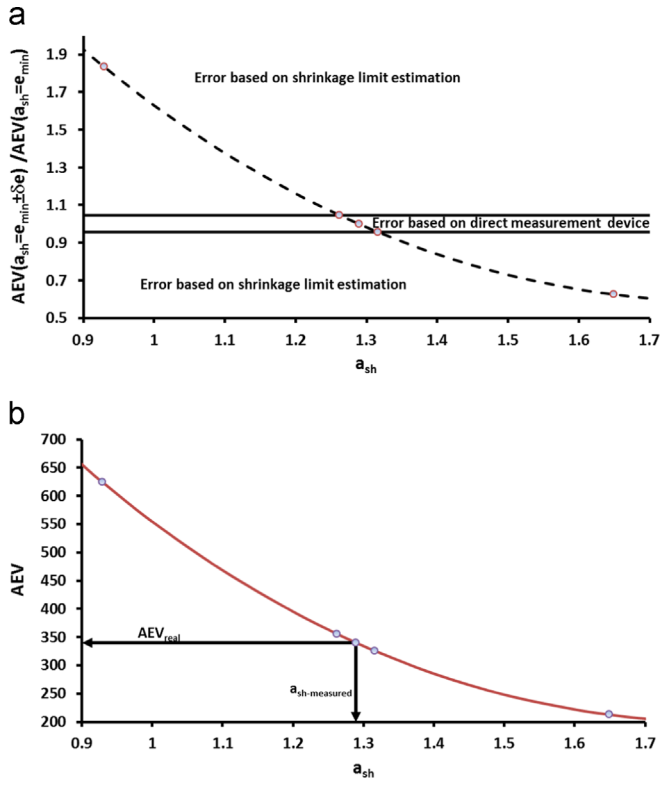

Fig. 18. Effect of a_{sh} on AEV. (a) Ratio of AEV due to difference in ash and (b) Variation of AEV due to difference ash values.

determined the shrinkage curves of vertisol and lixisol soil samples from Cuba using three different methods. The shrinkage curves were obtained using the direct measurement method of Berndt and Coughlan (1976), the balloon method (a volume displacement method) of Tariq and Durnford (1993) and the paraffin-coated method (a volume displacement method) of Lauritzen and Stewart (1942). The shrinkage curves using the balloon method and the paraffin-coated method were in good agreement; and therefore, only the data from the balloon method are used in this paper. As normal shrinkage is the subject of this paper, only the shrinkage curves for Vertizol A, B1, B2 and B3 are used in this paper. The shrinkage data of Cornelis et al. (2006) were in terms of moisture ratio υ, and no density of soil solids ρ_s was provided. Therefore, Eq. (1) is reformulated in terms of υ. Moisture ratio υ is defined as follows:

$$w = \upsilon \frac{\rho_w}{\rho_s} \tag{28}$$

and

$$b_{sh} = \upsilon_{SL'} \frac{\rho_w}{\rho_s} \tag{29}$$

where $\upsilon_{SL'}$ is

$$\upsilon_{SL'} = a_{sh} S_0 \tag{30}$$

Substituting Eqs. (28) and (29) into Eq. (1) gives

$$e(w) = a_{sh} \left[\frac{\upsilon^{C_{sh}}}{\upsilon_{SL'}{}^{C_{sh}}} + 1 \right]^{1/C_{sh}} \tag{31}$$

The soils were saturated before drying; therefore, $S_0 = 100\%$. Using $c_{sh} = 9$ and $a_{sh} =$ measured e_{min}, the estimated shrinkage curves for Vertisol A, B1, B2 and B3 are shown in Fig. 19. Fig. 19 shows that $a_{sh} = e_{min}$ and $c_{sh} = 9$ give a good estimate of the shrinkage curve. This shrinkage curve can then be used to construct the SWCC-*S* from the SWCC-*w*.

8. Proposed procedure to determine air-entry value of soils exhibiting shrinkage upon drying

Based on the above analyses and discussions, the air-entry value of soils should be determined from the SWCC-*S*. However, measuring the volume change in the soil specimens during the SWCC test is a tedious and unreliable task. Therefore, a procedure to estimate the air-entry value of the soils exhibiting shrinkage is proposed below:

1. Determine the SWCC-w from the SWCC test.
2. Air-dry the soil specimen at the end of the SWCC test to determine e_{min}.
3. Use $c_{sh} = 9$ and $a_{sh} = e_{min}$ in Eq. (1) to obtain the shrinkage curve. The value of b_{sh} is given by Eq. (2).
4. Use the SWCC-*w* and the shrinkage curve to obtain the SWCC-*S*.
5. Determine the AEV from the SWCC-*S* using either the graphical (Fig. 1) or the mathematical (Eq. (10)) method.

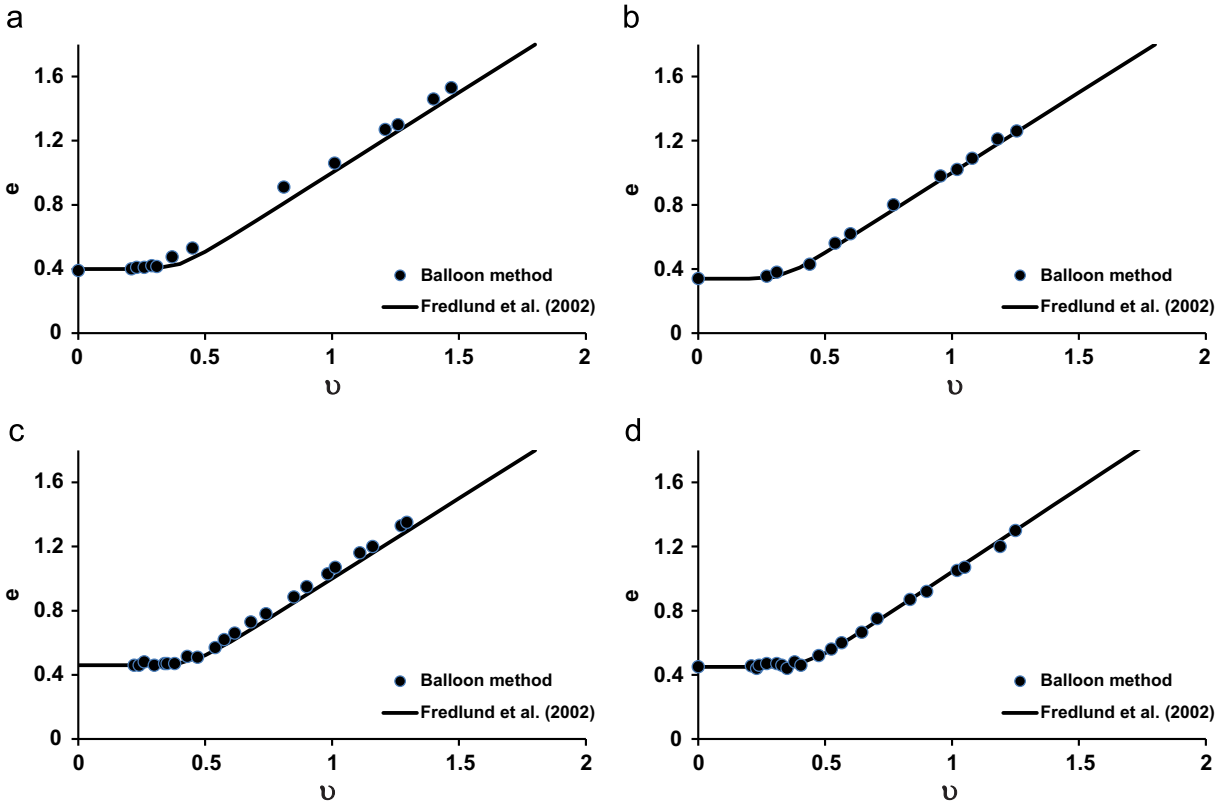

Fig. 19. Estimation of shrinkage curve using Eq. (31), $c_{sh}=9$ and $a_{sh}=$measured e_{min}. (a) Shrinkage curve of Vertisol A, (b) Shrinkage curve of Vertisol B1, (c) Shrinkage curve of Vertisol B2 and (d) Shrinkage curve of Vertisol B3.

9. Conclusion

The soil–water characteristic curves (SWCCs) of soils that shrink upon drying exhibit different air-entry values depending on whether the gravimetric water content, the volumetric water content or the degree of saturation is used as the ordinate. The correct air-entry value is given by the degree of saturation-based SWCC (SWCC-*S*). The SWCC-*S* can be estimated from the gravimetric water content-based SWCC (SWCC-*w*) and the shrinkage curve. A method to determine the shrinkage curve, using the final volume of a soil drying, was described. A procedure was proposed to determine the air-entry value of a soil exhibiting shrinkage upon drying.

Acknowledgement

The first author acknowledges the research scholarship from Nanyang Technological University, Singapore.

References

Adejumo, O.O., Balogun, F.A., 2012. Using the dual energy gamma-ray transmission technique to measure soil bulk density and water content of central southwestern Nigerian soils. J. Environ. Prot. **3** (**11**), 1409–1427. http://dx.doi.org/10.4236/jep.2012.311160.

ASTM D2435/D2435M, 2011. Standard Test Method for One-dimensional Consolidation Properties of Soils Using Incremental Loading. ASTM International, West Conshohocken, PA, 2011. http://dx.doi.org/10.1520/D2435_D2435M-11.

ASTM D4186 2006, 2006. Standard Test Method for One-dimensional Consolidation Properties of Saturated Cohesive Soils Using Controlled-strain Loading. ASTM International, West Conshohocken, PA, http://dx.doi.org/10.1520/D4186_D4186M-12.

ASTM D427 2004, 2004. Standard Test Method for Shrinkage Factors of Soils by the Mercury Method. ASTM International, West Conshohocken, PA, http://dx.doi.org/10.1520/D0427-04.

ASTM D4943-08 2008, 2008. Standard Test Method for Shrinkage Factors of Soils by the Wax Method. ASTM International, West Conshohocken, PA, http://dx.doi.org/10.1520/D4943-08.

ASTM D6836-02 2008, 2008. Standard Test Method for Determination of Soil Water Characteristic Curve for Desorption Using Hanging Column, Pressure Extractor, Chilled Mirror Hygrometer, or Centrifuge. ASTM International, West Conshohocken, PA, http://dx.doi.org/10.1520/D6836-02R08E02.

ASTM D4318-10 2010, Standard Test Methods for Liquid Limit, Plastic Limit, and Plasticity Index of Soils 2010, ASTM International; West Conshohocken, PA, http://dx.doi.org/10.1520/D4318-10.

Bao, C., Gong, B., Zhan, L., 1998. Properties of unsaturated soils and slope stability of expansive soils. In: Proceedings of the Second International Conference on Unsaturated Soils (UNSAT 98), International Academic, Beijing, China, 71-98.

Berndt, R.D., Coughlan, K.J., 1976. The nature of changes in bulk density with water content in a cracking clay. Aust. J. Soil Res. 15 (1), 27–37.

Brasher, B.R., Franzmeier, D.P., Valassis, V., Davidson, S.E., 1966. Use of saran resin to coat natural soil clods for bulk density and water retention measurement. Soil Sci. 101, 108. http://dx.doi.org/10.1097/00010694-196602000-00006.

Braudeau, E., Constantini, J.M., Bellier, G., Colleuille, H., 1999. New device and method for soil shrinkage curve measurement and characterization. Soil Sci. Soc. Am. J **63** (**3**), 525–535. http://dx.doi.org/10.2136/sssaj1999.03615995006300030015x.

BS 1377-2, 1990. Methods of Test for: Soils for Civil Engineering Purposes-Part 2. British Standards Institution.

Casagrande, A. 1932. Research of Atterberg Limits of Soils. Public Roads, 13, October 1932.

Chin, K.B., Leong, E.C., Rahardjo, H., 2010. A simplified method to estimate the soil–water characteristic curve. Can. Geotech. J. 47 (12), 1382–1400 (doi: 10.11 39/T10-033).

Cornelis, W.M., Corluy, J., Medina, H., Diaz, J., Hartmann, R., Van Meirvenne, M., Ruiz, M.E., 2006. Measuring and modelling the soil shrinkage characteristic curve. Geoderma 137 (1-2), 179–191. http://dx.doi.org/10.1016/j.geoderma.2006.08.022.

Fleureau, J.M., Verbrugge, J.C., Huergo, P.J., Correia, A.G., Kheirbek-Saoud, S., 2002. Aspects of the behaviour of compacted clayey soils on drying and wetting paths. Can. Geotech. J. Agric. Sci. 39 (6), 1341–1357 http://dx.doi.org/10.1139/t02-100.

Fredlund, D.G., 1964. Comparison of Soil Suction and One-dimensional Consolidation Characteristics of a Highly Plsatic Clay (M.Sc. Thesis). University of Alberta.

Fredlund, D.G., Rahardjo, H., Leong, E.C., Ng, C.W.W., 2001. Suggestions and recommendations for the interpretation of soil–water characteristic curves. In: Proceedings of 14th Southeast Asian Geotechnical Conference, Hong Kong, 503-508.

Fredlund, D.G., Stone, J., Stianson, J., 2011. Obtaining unsaturated soil properties for high volume change oil sands material. In: Proceedings of the Fifth Asia Pacific Conference on Unsaturated Soils-Pattaya, Thailand, Vol. 1, 415-420.

Fredlund, D.G., Stone, J., Stianson, J. 2011. Determination of water storage and permeability functions for oil sands tailings. In: Proceedings Tailings and Mine Waste, Vancouver, BC.

Fredlund, D.G., Xing, A., 1994. Equation for the soil–water characteristic curve. Can. Geotech. J. 31 (4), 521–532. http://dx.doi.org/10.1139/t94-061.

Fredlund, M.D., Wilson, G.W., Fredlund, D.G., 2002. Representation and estimation of the shrinkage curve. In: Third International Conference on Unsaturated Soils, UNSAT 2002, Recife, Brazil, March 10-13, 145-149.

Giráldez, J.V., Sposito, G., 1983. A general soil volume change equation: II. Effect of load pressure. Soil Sci. Soc. Am. J. 47 (3), 422–425. http://dx.doi.org/10.2136/sssaj1983.03615995004700030006x.

Giráldez, J.V., Sposito, G., Delgado, A., 1983. A general soil volume change equation: I. The two-parameter model. Soil Sci. Soc. Am. J 47 (3), 419–422. http://dx.doi.org/10.2136/sssaj1983.03615995004700030005x.

Goh, S.G., Rahardjo, H., Leong, E.C., 2010. Shear strength equations for unsaturated soil under drying and wetting. J. Geotech. Geoenviron. Eng. 136 (4), 594–606. http://dx.doi.org/10.1061/(ASCE)GT.1943-5606.0000261.

Guillermo, O.S., Roberto, R.F., Gimenez, D., 2001. Measurement of soil aggregate density by volume displacement in two non-mixing liquids. Soil Sci. Soc. Am. J. 65 (5), 1400–1403. http://dx.doi.org/10.2136/sssaj2001.6551400x.

Holtz, R.D., Kovacs, W.D, Sheahan, T.C., 2011. An Introduction to Geotechnical Engineering, second ed. Pearson Education, Inc., Upper Saddle River, NJ, USA.

Hunt, A.G., 2004. Comparing van Genuchten and percolation theoretical formulations of the hydraulic properties of unsaturated media. Vadose Zone J. 3 (4), 1483–1488. http://dx.doi.org/10.2136/vzj2004.1483.

Johnston, J.R., Hill, H.O., 1944. A case study of the shrinkage and swelling properties of Redzina soils. Soil Sci. Soc. Am. Proc. 9, 24–29.

Kayabali, K. 2012. Estimation of Liquid, Plastic, and Shrinkage Limit Using One Simple Tool. EJGE, 17. ⟨http://www.ejge.com/2012/Ppr12.174clr.pdf⟩ (accessed on 28 Dec 2013).

Khalili, N., Khabbaz, M.H., 1998. A unique relationship for χ for the determination of the shear strength of unsaturated soils. Géotechnique 48 (5), 681–687.

Kim, D.J., Vereecken, H., Feyen, J., Boels, D., Bronswijk, J.J.B., 1992. On the Characterization of Properties of an unripe marine clay soil. 1. Shrinkage processes of an unripe marine clay soil in relation to physical ripening. Soil Sci. 153 (6), 471–481. http://dx.doi.org/10.1097/00010694-199206000-00006.

Kohgo, Y. (2003). Review of constitutive models for unsaturated soils and initial-boundary value analyses. In: Proceedings of the Second Asian Conference on Unsaturated Soils, UNSAT-ASIA 2003, Osaka, pp. 21–40.

Kong, L.W., Tan, L.R., 2000. A simple method of determining the soil–water characteristic curve indirectly. In: Rahardjo, H., Toll, D.G. Leong, E.C. (Eds.), Unsaturated soils for Asia. In: Proceedings of the Asian Conference on Unsaturated Soils, UNSAT-Asia 2000, Singapore, A.A. Balkema, pp. 341-345.

Krisdani, H., Rahardjo, H., Leong, E.C., 2008. Effects of different drying rates on shrinkage characteristics of a residual soil and soil mixtures. Eng. Geol. 102 (1–2), 31–37. http://dx.doi.org/10.1016/j.enggeo.2008.07.003.

Lauritzen, C.W., 1948. Apparent specific volume and shrinkage characteristic of soils materials. Soil Sci. 65 (2), 155–179.

Lauritzen, C.W., Stewart, A.J., 1942. Soil-volume changes and accompanying moisture and pore–space relationships. Soil Sci. Soc. Am. Proc. 6 (C), 113–116. http://dx.doi.org/10.2136/sssaj1942.036159950006000C0 (019x).

Lee, I.M., Sung, S.G., Cho, G.C., 2005. Effect of stress state on the unsaturated shear strength of a weathered granite. Can. Geotech. J. 42 (2), 624–631.

Leong, E.C., Rahardjo, H., 1997. Review of soil–water characteristic curve equations. J. Geotech. Geoenviron. Eng. 123 (12), 1106–1117.

Liu, Q., Yasufuku, N., Omine, K., Hazarika, H., 2012. Automatic soil water retention test system with volume change measurement for sandy and silty soils. Soils Found. **52** (**2**), 368–380.

Mbonimpa, M., Aubertin, M., Bussière, B., 2006. Predicting the unsaturated hydraulic conductivity of granular soils from basic geotechnical properties using the modified Kovacs (MK) model and statistical models. Can. Geotech. J. 43 (8), 773–787. http://dx.doi.org/10.1139/t06-044.

McIntyre, D.S., Stirk, G.B., 1954. A method for determination of apparent density of soil aggregates. Aust. J. Agric. Res 5 (2), 291–296. http://dx.doi.org/10.1071/AR9540291.

Mitchell, A.R., 1992. Shrinkage terminology:escape from "normalcy". Soil Sci. Soc. Am. J. 56, 993–994.

Monnier, G., Stengel, P., Fies, J.C., 1973. Une methode de mesure la densite apparente de petits agglomerats terreuz. Application a l' analyse de systemes de porosite du sol. Ann. Agron 24, 533–545.

Peron, H., Hueckel, T., Laloui, L., 2007. An improved volume measurement for determining soil water retention curves. Geotech. Test. J. 30 (**1**), 1–8.

Philip, J.R., 1986. Linearized unsteady multidimensional infiltration. Water Resour. Res. 22 (**12**), 1717–1727. http://dx.doi.org/10.1029/WR022i012p01717.

Rassam, D.W., Cook, F.J., 2002. Predicting the shear strength envelope of unsaturated soils. Geotech. Test. J. 25 (**2**), 215–220. http://dx.doi.org/10.1520/GTJ11365J.

Rassam, D.W., Williams, D.J., 1999. Bearing capacity of dessicated tailings. J. Geotech. Geoenviron. Eng. 125 (7), 600–610. http://dx.doi.org/10.1061/(ASCE)1090-0241(1999)125:7(600).

Rijtema, P.E., 1965. An Analysis of Actual Evapotranspiration. Wageningen, Center for Agricultural Publications and Documentation.

Sibley, J.W., Williams, D.J., 1989. A procedure for determining volumetric shrinkage of an unsaturated soil. Geotech. Test. J. 12 (3), 181–187. http://dx.doi.org/10.1520/GTJ10966J.

SoilVision, 2003. SoilVision System Ltd. Saskatoon, Saskatchewan, Canada.

Sposito, G., Giraldez, J.V., 1976. Thermodynamic stanility and law of corresponding states in swelling soils. Soil Sci. Soc. Am. J. 40 (3), 352–358. http://dx.doi.org/10.2136/sssaj1976.03615995004000030016x.

Tariq, A., Durnford, D.S., 1993. Analytical volume change model for swelling clay soils. Soil Sci. Soc. Am. J. 57 (5), 1183–1187 (10.2136/sssaj1993.03615995005700050003x).

Tekinsoy, M.A., Kayadelan, C., Keskin, M.S., Soylemaz, M., 2004. An equation for predicting shear strength envelope with respect to matric suction. Comput. Geotech. 31 (7), 589–593. http://dx.doi.org/10.1016/j.compgeo.2004.08.001.

Thyagaraj, T., Rao, S.M., 2010. Influence of osmotic suction on the soil–water characteristic curves of compacted expansive clay. J. Geotech. Geoenviron. Eng. 136, 1695–1702.

Umezaki, T., Kawamura, T., 2013. Shrinkage and desaturation properties during desiccation of reconstituted cohesive soil. Soils Found. 53 (1), 47–63.

Watabe, Y., J.P., L.Please confirm that given name and surname has been identified correctly for author., Leroueil, S., 2006. Probabilistic modelling of saturated/unsaturated hydraulic conductivity for compacted glacial tills. Géotechnique **56** (**4**), 273–284. http://dx.doi.org/10.1680/geot.2006.56.4.273.

Xu, Y., 2004. Bearing capacity of unsaturated expansive soils. Geotech. Geol. Eng. 22 (**4**), 611–625. http://dx.doi.org/10.1023/B:GEGE.0000047043.29898.17.

Yule, D.F., Ritchie, J.T., 1980a. Soil shrinkage relationships of Texas Vertisols. 1. Small cores. Soil Sci. Soc. Am. J. 44 (6), 1285–1291. http://dx.doi.org/10.2136/sssaj1980.03615995004400060031x.

Yule, D.F., Ritchie, J.T., 1980b. Soil shrinkage relationships of Texas Vertisols. 2. Large cores. Soil Sci. Soc. Am. J. 44 (**6**), 1291–1295. http://dx.doi.org/10.2136/sssaj1980.03615995004400060032x.

Zhai, Q., Rahardjo, H., 2012. Determination of soil–water characteristic curve variables. Comput. Geotech. 42, 37–43. http://dx.doi.org/10.1016/j.compgeo.2011.11.010.

Zhan, L., Ping, C., NG, C, W.W.Please confirm that given name and surname has been identified correctly for author., 2007. Effect of suction change on water content and total volume of expansive clay. J. Zhejiang Univ. **8** (**5**), 699–706. http://dx.doi.org/10.1631/jzus.2007.A0699.